



Study of neuroprotective activity of new acetylcholinesterase inhibitors TVA and TVS in experimental model of Alzheimer's disease

Hrachik V. Gasparyan¹, Sona A. Buloyan¹, Hayk A. Harutyunyan², Anahit E. Pogosyan¹, Lilit M. Arshakyan¹, Lusine S. Harutyunyan¹, Zubeida A. Avetisyan³, Syuzanna R. Tosunyan¹, Armen A. Hovhannisyan¹, Vigen O. Topuzyan¹

1 *Scientific Technological Center of Organic and Pharmaceutical Chemistry, National Academy of Sciences of the Republic of Armenia, 26 Azatutian Ave., Yerevan 0014 Armenia*

2 *Yerevan State Medical University Named after Mkhitar Heratsi, 2 Koryun St., Yerevan 0025, Armenia*

3 *LA Orbeli Institute of Physiology National Academy of Sciences of the Republic of Armenia, 22 Orbeli Bros. St., Yerevan 0028, Armenia*

Corresponding author: Hrachik V. Gasparyan (hrachikgasparyan@mail.ru)

Academic editor: Mikhail Korokin ♦ **Received** 6 June 2022 ♦ **Accepted** 24 October 2022 ♦ **Published** 29 November 2022

Citation: Gasparyan HV, Buloyan SA, Harutyunyan HA, Pogosyan AE, Arshakyan LM, Harutyunyan LS, Avetisyan ZA, Tosunyan SR, Hovhannisyan AA, Topuzyan VO (2022) Study of neuroprotective activity of new acetylcholinesterase inhibitors TVA and TVS in experimental model of Alzheimer's disease. *Research Results in Pharmacology* 8(4): 77–88. <https://doi.org/10.3897/rrpharmacology.8.87431>

Abstract

Introduction: Alzheimer's disease (AD) is a severe neurodegenerative disease characterized by loss of synaptic connection between neurons of the cortex and subcortical regions. The cholinergic deficit is a consistent and early finding in AD, hence acetylcholinesterase inhibitors (AChEIs) are used for symptomatic improvement of AD. Most of these therapeutic agents are hepatotoxic, leading to liver failure and other complications. Therefore, the study of new AChEIs with less toxic impact and better effectivity is a topical challenge. In view of this, we synthesized novel chemical compounds: TVA and TVS that possess AChEI activity and studied their neuroprotective effect in an experimental AD model.

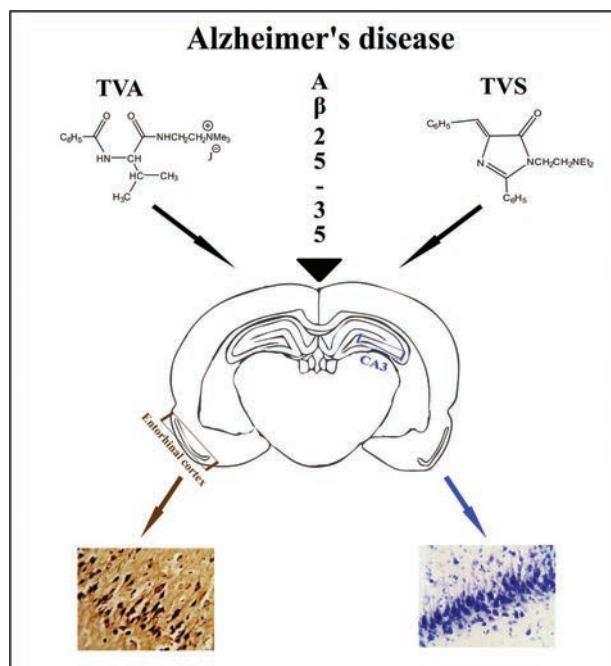
Materials and methods: Studies were performed on white rats. Acute toxicity studies were performed by Karber's method. AD was induced via bilateral intracerebroventricular administration of A β 25–35. Histopathological examinations were performed in the hippocampus and the entorhinal cortex. Liver tissue was additionally examined to monitor the hepatotoxicity of these compounds.

Results: Studies of the hippocampus showed that compared to control and TVA-treated groups, under the influence of TVS there were few morphological alterations. Experimental groups showed an increase in the glial cell count, compared to the intact animals. In comparison to the AD group, the increase in microglia was not that prominent under the action of the novel compounds. Under the influence of TVA and TVS, the entorhinal cortex was more susceptible to neuronal injury, although TVS protected pyramidal neurons. Also, the group treated with TVA had signs of acute liver damage, while under the influence of TVS there were no signs of liver changes.

Discussion: Histopathological examination showed that the neurodegenerative processes in the hippocampus, as well as in the entorhinal cortex, were significantly reduced under the influence of TVS, compared with the control group. At the same time, TVA had no significant effect on the protection of neuronal cells. Also, TVS was less toxic, and there was no sign of hepatotoxicity during the experiments.

Conclusion: These studies demonstrated that TVS possesses neuroprotective activity and reduces neuronal damage induced by A β .

Graphical abstract



Keywords

acetylcholinesterase inhibitors, acute toxicity, entorhinal cortex, hippocampus, histopathological examination, neuroprotection.

Introduction

Alzheimer's disease (AD) is a progressive and fatal neurodegenerative disorder that leads to cognitive and memory loss and an increasing impairment of daily activities, as well as a variety of neuropsychiatric symptoms (Mufson et al. 2008). It was established that neurofibrillary degeneration of the neurons' cholinergic nucleus basalis of Meynert, designated Ch4, is present at the early stages of AD (Mesulam et al. 2004). Serious loss of cholinergic function in the central nervous system contributes to the cognitive symptoms of AD (Bartus et al. 1982). As the cholinergic deficit is a consistent and early finding in AD, acetylcholinesterase (AChE) is still considered as one of the viable therapeutic targets for symptomatic improvement of this disease (Bartus et al. 1982; Mufson et al. 2008; Mehta et al. 2012; Hampel et al. 2019). Hence acetylcholinesterase inhibitors (AChEIs), such as donepezil, rivastigmine, and galantamine, were developed and approved for the treatment of AD (Tabet 2006). Although they were approved for use in AD, these drugs have limited therapeutic efficacy, and long-term intolerance, due to poor bioavailability, hepatotoxicity, and non-selectivity (Agatonovic-Kustrin et al. 2018). Also, the adverse effects of AChEIs are associated with an increase in peripheral cholinergic signaling and often mirror activation of the parasympathetic nervous system (Bloemer 2020). Hence the search for and development of new therapeutic agents remains an ongoing challenge.

Although the key factors in the development of AD are the beta-amyloid ($\text{A}\beta$) and abnormal tau protein, oxidative damage and a slow inflammatory process are two possible mechanisms involved in it (McGleenon et al. 1999). Inflammatory pathways are increasingly recognized as essential contributors to cell death in AD (Stuchbury and Münch 2005). It was shown that AChEIs directly inhibit the release of cytokines from microglia and monocytes and have an anti-inflammatory effect in the brain as well (Tabet 2006). There is multiple evidence that improvement of AD with AChEIs may be achieved independently of an acetylcholine raise, and possibly these agents might offer a degree of neuroprotection in AD because of their anti-inflammatory effect (Francis et al. 2005). Due to these effects of AChEIs, new derivatives with the same or better efficacy and lesser side effects are in development (Bartus et al. 1982; Makarian et al. 2022).

From this perspective, compounds such as N-substituted amino acids dialkylaminoalkylamides are of special interest as they display acetylcholinesterase inhibitor activity (Abbasi et al. 2014). We have synthesized the novel compounds: N-benzoyl-DL-valinedimethylamino-ethylamine iodmetilate (TVA) and 1-diethylaminoethyl-2-phenyl-4-benzylidene-5-imidazolone (TVS), possessing prominent anticholinesterase and antibutrylcholinesterase activity (Topuzyan et al. 2018). Thereafter, in this paper, we study their neuroprotective effects in rodent AD models, as well as report toxicological studies of these compounds.

Materials and methods

Synthesis of chemical compounds

Compound TVA was synthesized by the method of active esters. The oxibenzotriazolic ester of N-benzoyl-DL-valin (III) was synthesized using esthered reagent o-nitrophenylsulfonyloxybenzotriazole (II). The resulting compound III, without separation from the mixture, was reacted with dialkylamino alkyl amines. The obtained dimethylaminoethyl amid of N-benzoyl-DL-valin was reacted with methyl iodide and turned to quaternary ammonium salt (Fig. 1).

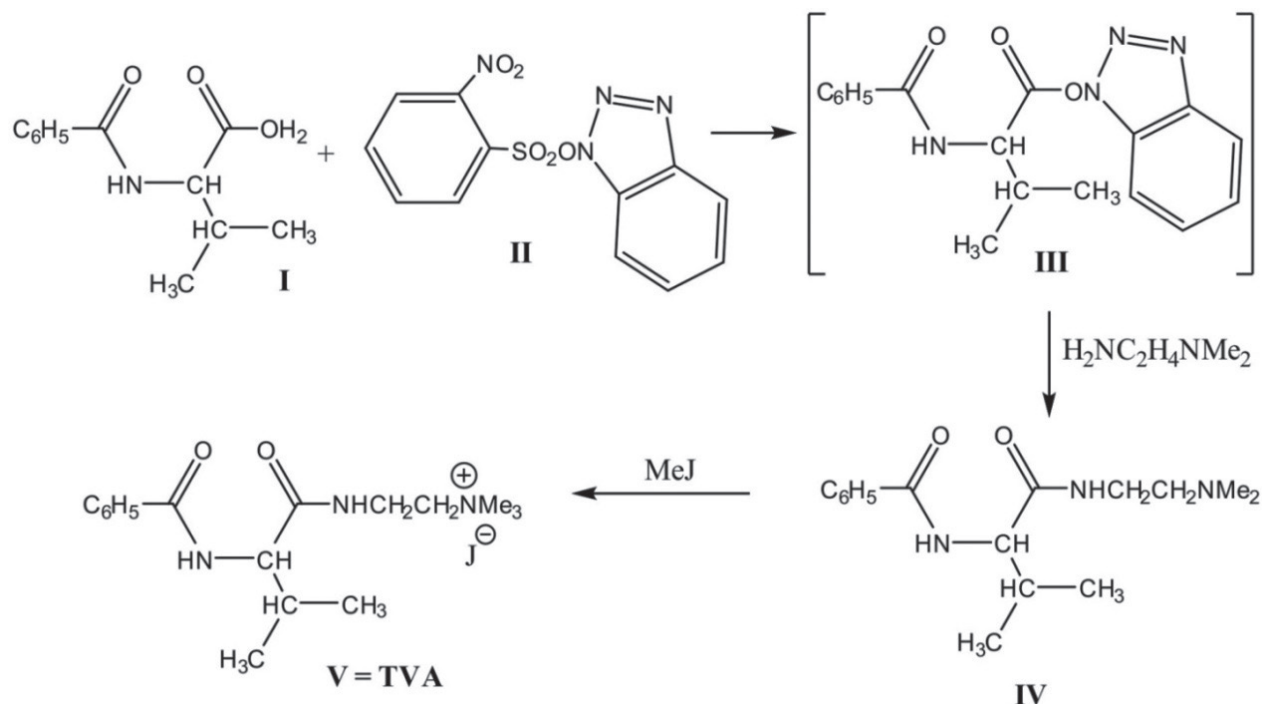


Figure 1. Synthesis of N-benzoyl-DL-valinedimethylamino-ethylamine iodmetilate (TVA).

The synthesis of the second compound, TVS, was achieved by the azlactone method. 2-phenyl-4-benzylidene-5 oxazolone (VI) was reacted with 2-diethylaminoethanol (VII), and the obtained N-benzoyl- α,β -dehydrophenilalaninediethylamino ethyl amide (VIII) was cyclized with hexamethyldisilazane (Fig. 2) (Topuzyan et al. 2018).

Animals

Animal experiments were performed in compliance with Directive 2010/63/EU, with the approval of the Bioethical Committee of Mkhitar Heratsi Yerevan State Medical University (minutes №1-8/2020). They were placed in a room at 21 ± 2 °C, and 12 hours diurnal cycle with humidity levels 40–43%. Food and water were given ad libitum. Three animals of the same sex were placed in cages of 1600 cm².

Acute toxicity test

Acute toxicity studies by Karber's method were performed on outbred white rats weighing 180–200 g (Chinedu et

al. 2013). Compounds TVA and TVS, dissolved in distillate water (Tween 80, E433), were administered once via intraperitoneal injection in various doses. Each group consisted of five male and five female animals. In the first series, the LD_{100} dosage was determined, the least dose being with 100% animal mortality. In the second series, the maximum tolerated dose (MTD) of the compounds with no animal mortality was determined. Between these two, we selected two interval doses and tested them in the same way. The mortality rate was recorded in each group. The gross observable clinical and behavioral changes in the animals were examined 15, 30, 45, 60 and 90 minutes

after the initial injection and for 14 days of the experiment. The LD_{50} was calculated through Karber's arithmetical method, as follows:

$$\text{LD}_{50} = \text{LD}_{100} - \sum \left(\frac{a \times b}{n} \right)$$

where LD_{50} = median lethal dose; LD_{100} = least dose required to kill 100%; a = dose difference; b = mean mortality; n = group population.

Design of AD experiment

Studies were performed on outbred male white rats, weighing 200–250 g. The animals were divided into four groups (n = 6): a) Intact group – normal animals; b) Experimental AD group – non-treated animals with AD induced by A β 25–35; c) Experimental group I – animals treated with TVA, after A β 25–35 administration; d) Experimental group II – animals treated with TVS, after A β 25–35 administration.

AD was induced via bilateral intracerebroventricular administration of 3 μl 10^{-9} M A β 25–35 (Sigma-Aldrich,

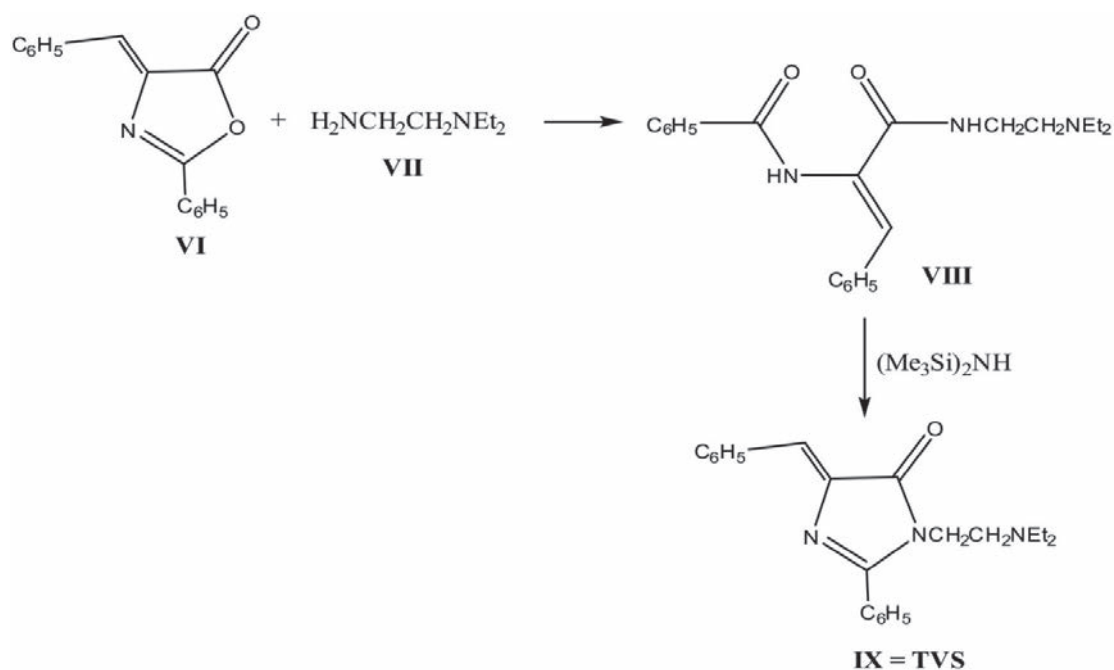


Figure 2. Synthesis of 1-diethylaminoethyl-2-phenyl-4-benzylidene-5-imidazolone (TVS).

USA) (Maurice et al. 1998). Prior administrations of 1 mg/ml of A β 25–35 were aggregated for 4 days at 37 °C. Intracerebroventricular administration of the toxic oligomer A β 25–35 was made under general anesthesia (Ketamine/Xylazine 80/10 mg/kg via intraperitoneal injection) according to the stereotaxic atlas coordinates (AP–1, L \pm 1.5, DV+3.5 mm) (Paxinos and Watson 2005). TVA and TVS were administered via intraperitoneal injection in 20 mg/kg dosage 14 times over one month. After the final injection, the animals were left for 12 weeks for the recovery period.

Histopathological observation

After the recovery period, the rats were sacrificed under anaesthesia (40 mg/kg Nembutal via intraperitoneal injection). Brain and liver tissue was collected and stored in 10% buffered formalin. Samples were dehydrated, embedded in paraffin, and 3–5 μ m microtome sections were prepared. Brain sections were stained with Nissl and Bielschowsky silver stain, liver tissue – with H&E (Sigma-Aldrich, USA) (Korjevski and Gliyarov 2010), and examined with a light microscope.

Morphometric analysis

Ten samples of the entire hippocampal CA3 region with Nissl stain were photographed at 100 \times magnification via AmScope MU500 5MP USB2.0 Microscope Digital Camera & Software (USA). For differentiation of morphological features, photomicrographs were additionally magnified by ImageJ 1.x software. Normal neurons with a light nucleus, dark pyknotic neurons, and chromatolytic neurons were counted by using Cell Counter Plugin. For glial cells, additional ten images were obtained at 400 \times magnification. Microglial and astroglial cells of the CA3 region were counted within microscopic field.

Statistical analysis

All data were expressed as means \pm S.D. Statistical analysis of data was performed using IBM SPSS Statistics 22.0.0 software with one-way ANOVA, with Levene test for equality of variances followed by nonparametric Games-Howell post hoc test.

Results

Acute toxicity test

The acute toxicity test of TVA showed the LD₁₀₀ dosage of this compound at 350 mg/kg, whereas the MTD was 50 mg/kg. The 2 interval dosages were 100 mg/kg and 200 mg/kg. Observation during the 15–90 minutes after injection showed that the animals experienced the dose-dependent onset and severity of toxic symptoms. Gross observable symptoms of LD₁₀₀ dosage constituted severe convulsions, dyspnea, and an increased heart rate of animals. After 30 minutes, all the animals died. In the case of intermediate dosage, within 90 minutes of observation, the animals were mainly lethargic, with shallow breathing and mostly no response to external triggers. At the MTD dosage, the animals were mostly passive, but responsive to external triggers after 45 minutes following the injection. After 60 minutes of the experiment, the animals regained normal activity and started to use food and water. Between the 1st and the 14th days of observation, the condition of all survivors was normal, without noticeable behavioral and physiological changes. The animals were using food and water. The mortality rate is presented in Table 1. The LD₅₀ of TVA was 218 mg/kg by the Karber calculation.

The same test for TVS determined that LD₁₀₀ was 1000 mg/kg, MTD was 125 mg/kg, and interval dosages

Table 1. Mortality after injection of various doses of compound TVA

Dosage	350 mg/kg	200 mg/kg	100 mg/kg	50 mg/kg
Survival	No survivors	6 animals	9 animals	10 animals
Death	10 animals	4 animals (3♀; 1♂)	1 animal (1♀)	No mortality

were 250 and 500 mg/kg. At LD_{100} , after 15 minutes of the experiment, the animals experienced severe convulsions with shallow irregular breathing and tachycardia. After 30–60 minutes, the animals were lethargic with shallow breathing and gradually died from intoxication. The last one died after 90 minutes. With intermediate dosages, after 15 minutes following the injection, the animals had moderate convulsions and were in a lethargic state. After 30–60 minutes of the experiment, convulsions intensified. The animals had dyspnea, and their eyes were half-opened. After 90 minutes, the survivors were passive, but responsive to external triggers. Several animals were using food and water. At MTD dosage after 45 minutes following the injection, the animals were mostly passive, but responded to external triggers. The breathing rate was normal. After the 60 minutes of the experiment, the animals became active and started to use food and water.

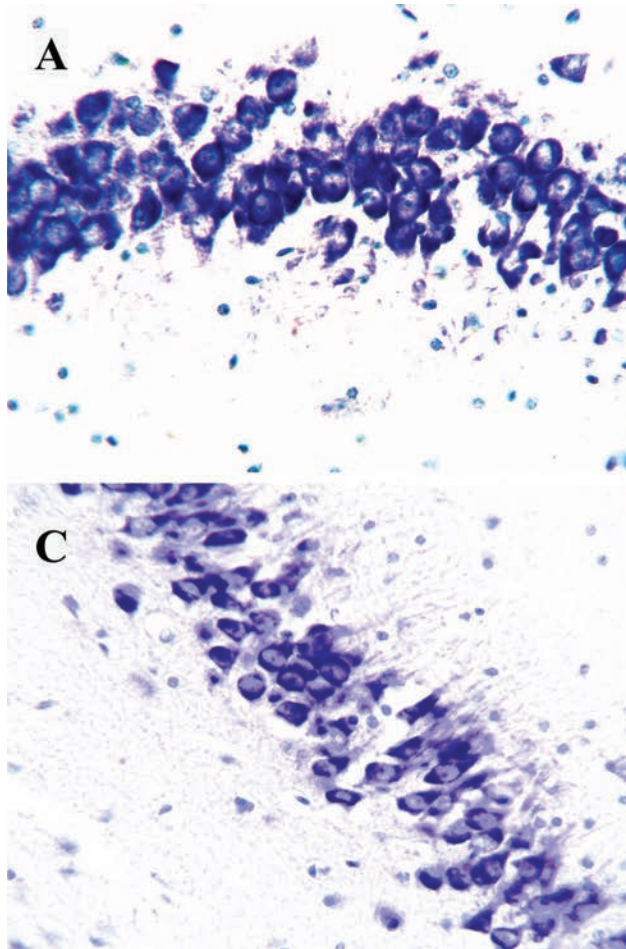


Figure 3. Photomicrographs of CA3 hippocampal region stained with Nissl stain $\times 400$. **A.** Intact animals: The neurons are neatly arranged with a clear nucleus and visible nucleoli; **B.** Animals with AD induced by $A\beta$ 25–35: cells have dark pyknotic appearance, with indistinct nucleus; **C.** Animals treated with TVA: neurons are arranged scantily, the cytoplasm was stained in different shades; **D.** Animals treated with TVS: there are few dark pyknotic neurons, mostly with a clear nucleus, cytoplasm has visible Nissl bodies.

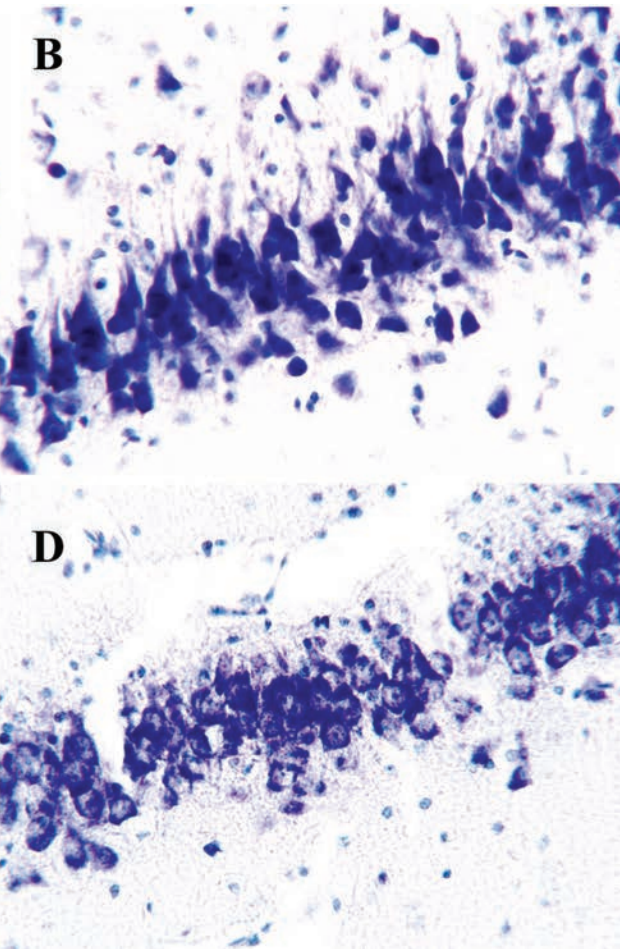
Table 2. Mortality after injection of various doses of compound TVS

Dosage	1000 mg/kg	500 mg/kg	250 mg/kg	125 mg/kg
Survival	No survivors	5 animals	8 animals	10 animals
Death	10 animals	5 animals (3♀; 2♂)	2 animals (2♂)	No mortality

The mortality rate is presented in Table 2. LD_{50} of TVS was 525 mg/kg.

Histopathological observation and morphometric analysis

Morphological observation with Nissl stain and morphometric analysis of brain tissue showed no noticeable histological alterations in the intact animals. The neuronal cells of the CA3 region were neatly arranged and displayed sharp edges (Fig. 3A). From the total of 141 ± 6.164 cells in the microscopic field, normal cells were 120.4 ± 5.892 , whereas only a few cells had dark pyknotic (12.8 ± 0.919 cells) or chromatolytic (7.8 ± 1.398 cells) appearance (Fig. 4). There were very few microglial cells (10 ± 1.247 cells) in this region and astrocytes (18.9 ± 2.846) accounted for most of the glial cells (Fig. 5).



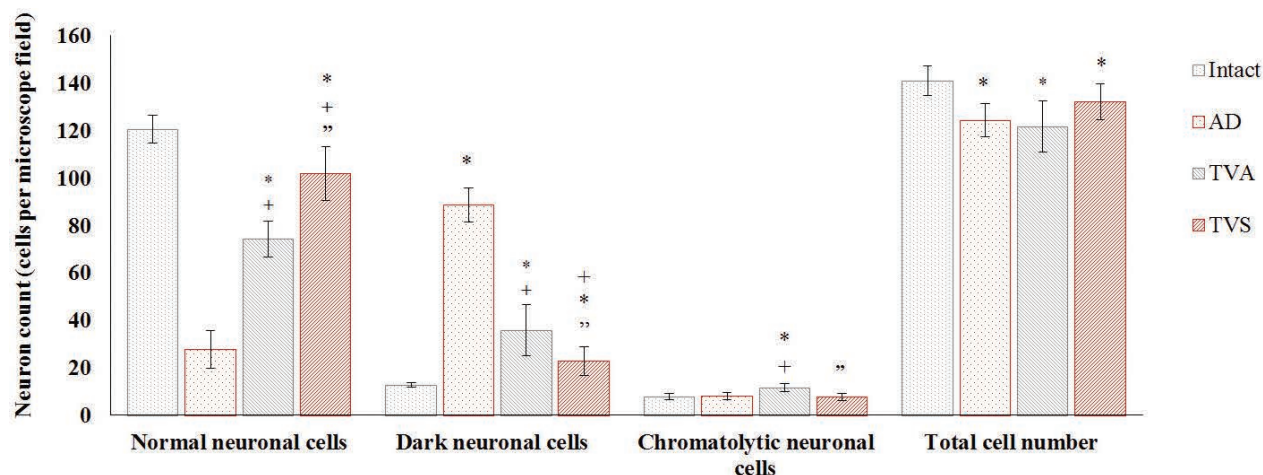


Figure 4. The count of neuronal cells in CA3 hippocampal region. **Note:** Data is expressed as Mean \pm SD; * – $p < 0.05$ compared with the intact group; + – $p < 0.05$ compared with the AD group; ++ – $p < 0.05$ compared with the group treated with TVA.

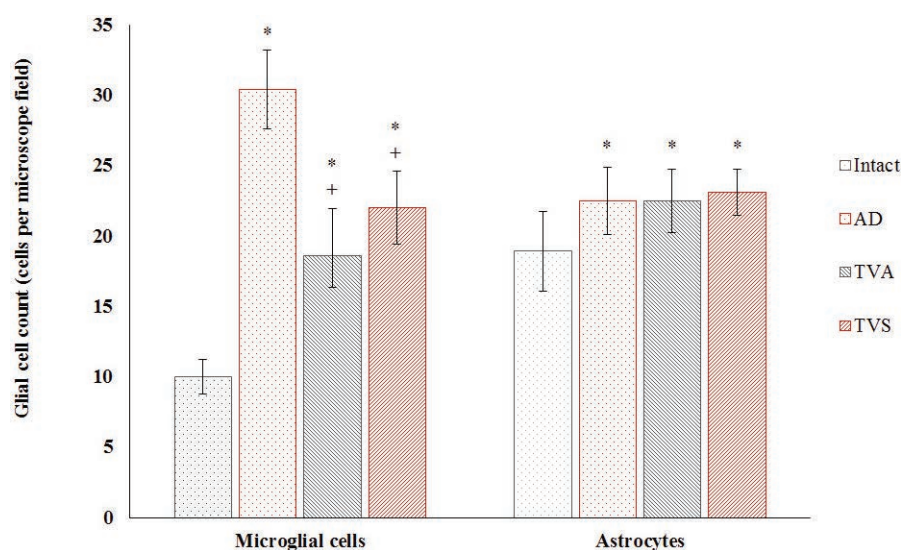


Figure 5. The count of glial cells in CA3 hippocampal region. **Note:** Data is expressed as Mean \pm SD; * – $p < 0.05$ compared with the intact group; + – $p < 0.05$ compared with the AD group.

After administration of A β 25–35 in the untreated AD group, there were prominent morphological changes in the hippocampal CA3 region (Fig. 3B). Examination showed severe degeneration of neuronal cells, where the majority of cells displayed dark pyknotic appearance with missing or indistinct nucleoli (88.6 ± 7.027 cells, $P < 0.05$). There was a significant decrease in neuronal cell count in this group (124.3 ± 6.993 cells, $P < 0.05$), and the majority of cells were dark neurons, whereas the count of chromatolytic cells (8 ± 1.633) was not significantly different from that in the intact animals (Fig. 4). Under the deposition of A β , there was prominent gliosis, and vacuolization in the microscopic field. The count of microglial cells drastically increased and amounted to 30.4 ± 2.797 cells in the microscopic field ($P < 0.05$). The astrocyte count also significantly increased and amounted to 22.5 ± 2.369 cells in the microscopic field ($P < 0.05$) (Fig. 5).

Almost the same histological alterations were observed in the group treated with TVA (Fig. 3C), where the number of normal cells (74.2 ± 7.685 cells), as well as the total number of cells (121.7 ± 10.761), decreased compared to

that in the intact group ($P < 0.05$). However, the count of normal neuronal cells was significantly higher compared to that in the AD group ($P < 0.05$), whereas the total number of cells was not significantly lower. In this group, the numbers of chromatolytic cells (11.6 ± 1.776 cells) were significantly higher compared to those in the intact and AD animals (Fig. 4). Compared to the intact animals, there was evidence of gliosis in this group. The count of microglial cells also increased (18.6 ± 3.373 cells), although the number of cells was significantly lower compared to that in the the AD group ($P < 0.05$). Astroglial cell count was also higher compared to that in the intact animals and consisted of 22.5 ± 2.273 cells in the microscopic field ($P < 0.05$) (Fig. 5).

Compared to the previous group, under the influence of TVS, the morphological state of the hippocampus more resembled the normal animals, and the neuronal cells were fairly intact with visible Nissl bodies in the cytoplasm (Fig. 3D). Although the number of normal cells (101.8 ± 11.371) significantly reduced compared to that in the intact group ($P < 0.05$), it was significantly higher than

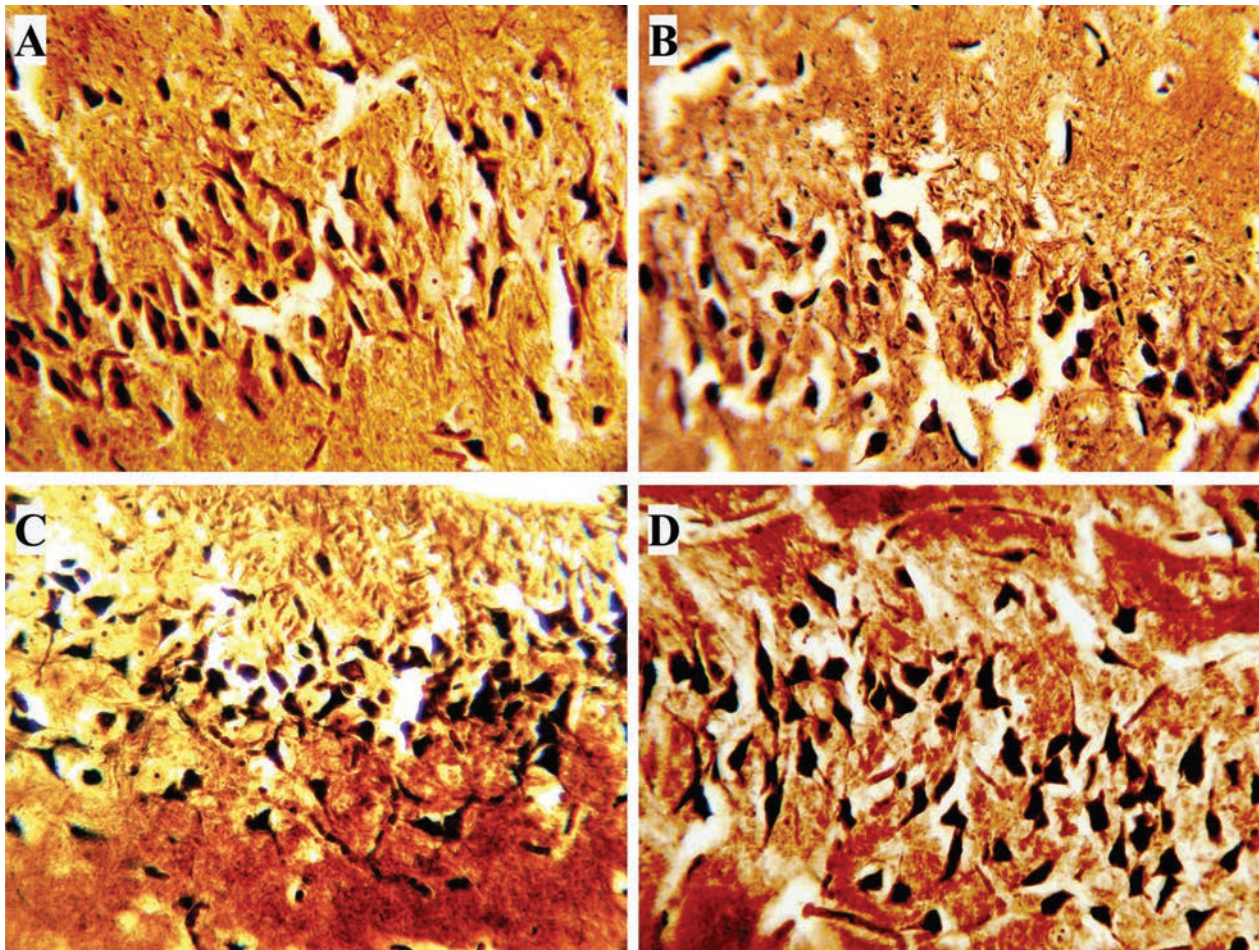


Figure 6. Photomicrographs of CA3 hippocampal region stained with Bielschowsky silver stain $\times 400$. **A.** Intact animals: numerous pyramidal cells mostly with light brown cytoplasm, no sign of extracellular precipitations; **B.** Animals with AD induced by A β 25–35: shrinkage of pyramidal neurons, some neurons have elongated flamed-shaped filament aggregates in the perikaryon (neurofibrillary tangles), determined slight extracellular precipitation; **C.** Animals treated with TVA: degenerative vacuolization of neurons, elongated flamed-shaped filament aggregates within the perikaryon; **D.** Animals treated with TVS: there are visibly more viable neurons in the region, as well as vacuolization and flamed-shaped filament aggregates in the neurons.

in the non-treated group and the group treated with TVA ($P < 0.05$). There were fewer dark pycnotic cells (22.8 ± 6.161) compared to the AD group ($P < 0.05$) and the TVA treated animals ($P < 0.05$). Also, the number of chromatolytic cells (7.6 ± 1.506) was significantly lower compared to that in the TVA treated animals ($P < 0.05$). The total number of neuronal cells was 132.2 ± 7.525 in the microscopic field, insignificantly higher than in other experimental groups (Fig. 4). There was mild gliosis in this group. The count of microglial cells was 22 ± 2.582 cells, which is significantly lower than in the AD group ($P < 0.05$). Along with that, the astroglial count was not so different from that in other experimental groups (23.1 ± 1.663 cells) (Fig. 5).

The histopathological observation of brain tissue stained with Bielschowsky silver stain showed a picture more or less similar to the previous examination. In the AD group, after amyloid administration, there were numerous dark brown deposits in the hippocampus (Fig. 6B), as well as in the entorhinal cortex (Fig. 7B). In contrast, in the intact animals, there was no sign of amyloid plaque formation (Figs. 6, 7A). There was shrinkage of the hippocampus pyramidal neurons in the animals of the AD

group, and numerous neurofibrillary tangle-like structures (Fig. 6B). In the cortex, the depositions of plaque-like structures were more prominent. There were few pyramidal neurons in the III layer of the entorhinal cortex, besides, in I, II, and III layers of the cortex there was degenerative vacuolization, as well as prominent neurofibrillary tangles in the neurons of the II layer (Fig. 7B).

In the groups treated with TVA and TVS, brain tissue morphological pictures were similar to those in the AD group, where the neurons had undergone degenerative vacuolization; also deposition of senile plaques and neurofibrillary tangle was observed (Figs 6, 7C, 7D). Nevertheless, under the influence of TVS, there were more viable cells in the hippocampus (Fig. 6D) compared to those in the AD animals. The pyramidal neurons in III layer of the entorhinal cortex were preserved compared to those in the AD and TVA treated groups (Fig. 7D). In the group treated with TVA, the hippocampus had shown morphological alterations similar to those in the group treated with TVS (Fig. 6C). Still, in the entorhinal cortex, there were few viable cells throughout cortical layers (Fig. 7C).

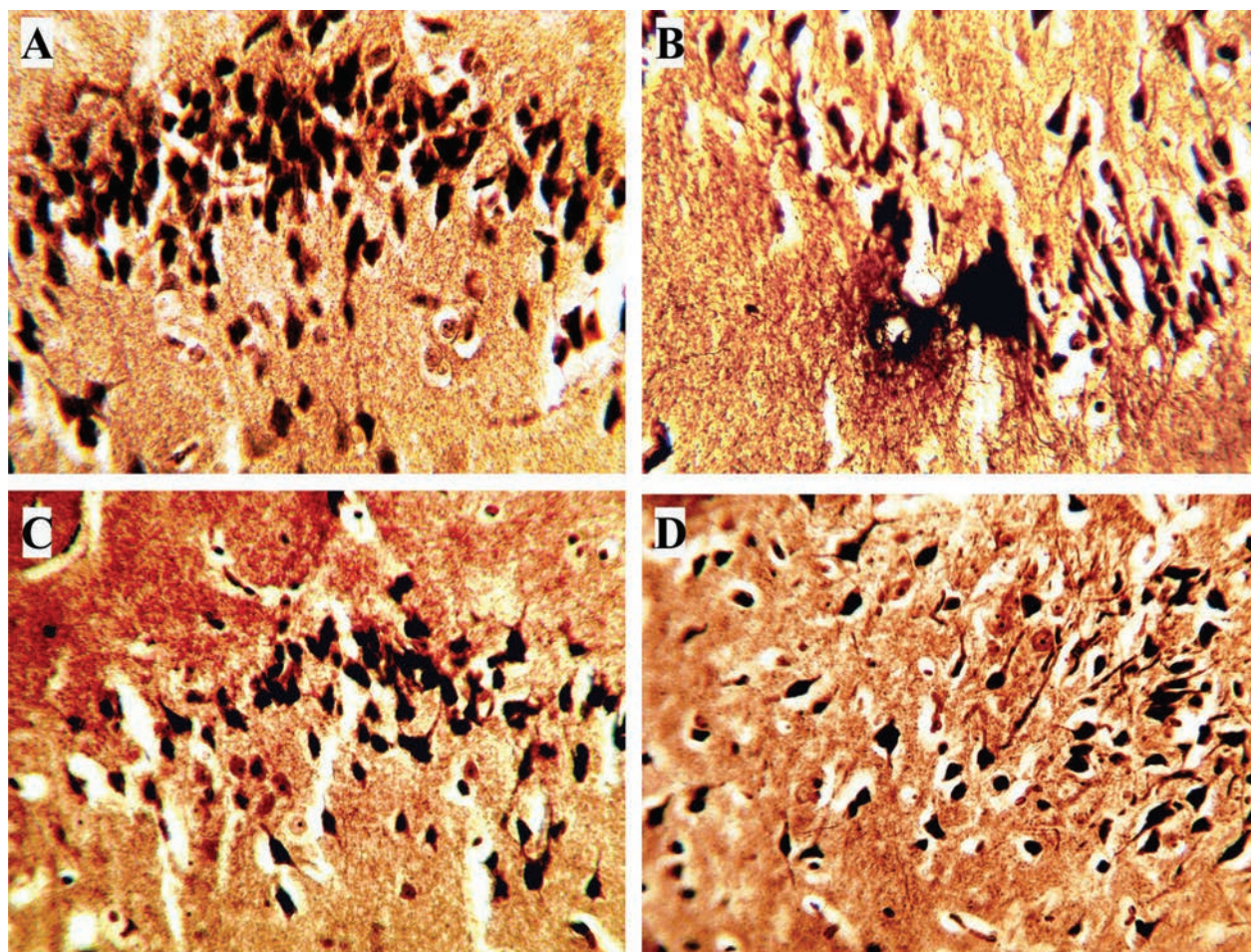


Figure 7. Photomicrographs of entorhinal cortex stained with Bielschowsky silver stain $\times 100$, $\times 400$. **A.** Intact animals: hyperchromatic islets of round neurons in II layer and medium-size pyramidal cells of III layer; **B.** Animals with AD induced by A β 25–35: depositions of plaque-like structures, II layer has few neurons and most of them are vacuolized and have flamed-shaped filament aggregates in the perikaryon; **C.** Animals treated with TVA: reduced amount of the cells in cortical layers, flamed-shaped filament aggregates in the perikaryon; **D.** Animals treated with TVS: III layer viable cells dominate, on II layers most cells have flamed-shaped filament aggregates in the perikaryon.

Histopathological observation of liver tissue showed that in the untreated animals there were fatty changes and pycnosis of hepatocytes; however, there were no signs of acute intoxication and periportal inflammation in this group (Fig. 8B). While in the group treated with TVA, there were prominent acute inflammatory processes in portal tracts with neutrophil infiltration and necrosis of hepatocytes, without prominent fatty changes (Fig. 8C). In comparison, there were no noticeable morphological changes in liver tissue, and liver structure resembled that of the intact animals in the group treated with TVS (Fig. 8A, D).

Discussion

As compounds TVA and TVS were novel and had not been used for therapeutic purposes, before studying their neuroprotective activity, we conducted an acute toxicity test to obtain information about LD₅₀, therapeutic index, and the safety degree of a pharmacological agent (Akhila

et al. 2007). The acute toxicity test showed that TVS was more than twice less toxic than TVA, thus safer for therapeutic purposes. Pursuant to the results of this test, we decided preliminarily to use the same therapeutic dosage for these compounds, which was around ten times lower than LD₅₀ of TVA. Therefore 20 mg/kg was used as an initial therapeutic dosage of compounds TVA and TVS.

In the AD patients with mild cognitive impairment and in experimental models in CA3 region, there is hyperactivity and hyperinduction of AD-related proteins. Studies showed that at an early stage of AD, before the deposition of β amyloid plaques, the synaptic plasticity between the dentate gyrus and CA3 was markedly impaired (Zhang et al 2013; da Silva et al. 2019). Therefore, in this study Nissl stain was used to identify Nissl bodies and extend neuronal damage in the hippocampus CA3 region which contains pyramidal cells. This method can reveal the characteristic morphological alteration of chromatolysis, which is a reactive change occurring in the cell body of damaged neurons, involving the dispersal and redistribution of Nissl bodies (Bradley et al. 2018). Another typical morphologi-

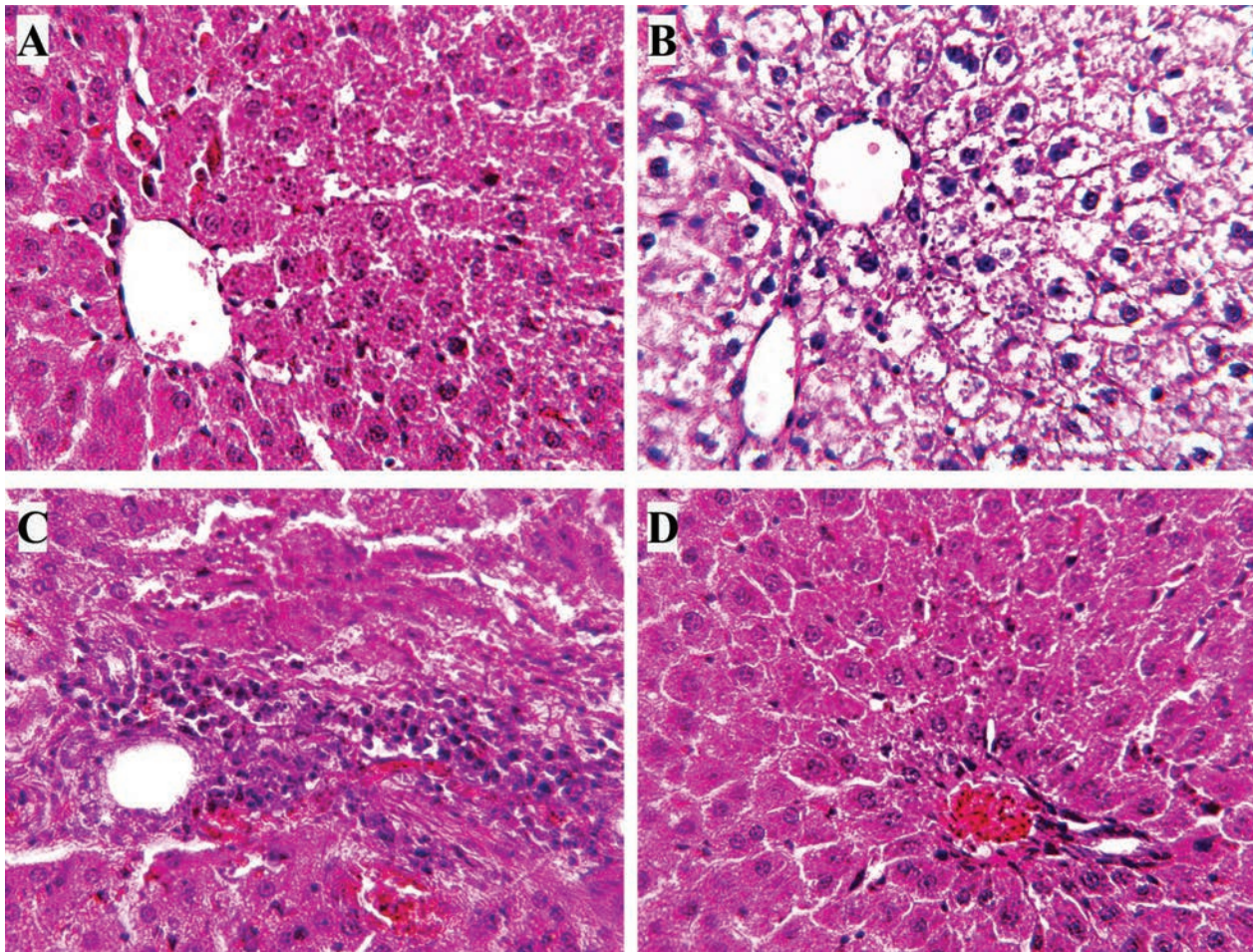


Figure 8. Photomicrographs of liver tissue stained with H&E $\times 400$. **A.** Intact animals: the structure is preserved, hepatocytes are distinguished with a clear nucleus; **B.** Animals with AD induced by $A\beta$ 25–35: foamy hepatocytes with microvesicular steatosis; **C.** Animals treated with TVA: neutrophil infiltration around portal tracts, hepatocytes are with pyknotic nuclei; **D.** Animals treated with TVS: the structure of liver tissue is preserved, without noticeable infiltrative processes.

cal change is dark neurons that occur in many stroke types, such as traumatic brain injury, which may be observed through various staining methods, such as H&E, Nissl, and silver stain (Ooigawa et al. 2006). Since in the AD group the majority of hippocampal cells were dark pycnotic, and there was prominent gliosis, in the morphometric analysis after $A\beta$ 25–35 administration, we counted normal, dark, and chromatolytic neuronal cells. In our experiments, few amounts of these dark pycnotic cells were observed in the hippocampus of the intact animals as well, but as there were no signs of microglial activation and vacuolization of neurons, we considered them as common artifacts related to pressure on fresh rat brain at necropsy (Jortner 2006). The increase in the dark cell count in all the experimental groups can be explained by the extracellular deposition of β -amyloid that also promotes oxidative stress on neurons (Behl et al. 1994). Studies with Nissl stain have shown that compared to the control and TVA-treated groups, under the influence of TVS, there were few morphological alterations. The total of neuronal cells of this group was no different from the norm. TVA did not show noticeable differences from the control animals, and damaged neuronal cells were higher in the count.

Studies of the pathogenesis of AD showed that there are numerous reactive astrocytes and microglia within the neuritic plaques and in the vicinity of the $A\beta$ deposits (Hemnonot et al. 2019). Recent studies suggest that in AD microglial activation acts as a bridge leading to the pathological phosphorylation and aggregation of tau (Dani et al. 2018). On the one hand, in the brains of patients with AD, microglia is closely located to amyloid plaques; on the other, tau load and microglial cell load have also been described in post-mortem and in vivo neuroimaging studies (Hayes et al. 2002; Dani et al. 2018; Leng and Edison 2021). In our studies, experimental groups showed an increase in glial cell count, compared to that in the intact animals. The microglial count was very high in the AD group; in comparison, an increase in microglia was not that prominent under the action of novel compounds. The increase in the astroglial cell count was the same in all the experimental groups. A possible neuroprotective effect of AChEIs may be the cholinergic anti-inflammatory action by stimulating anti-apoptotic pathways in glial cells (Benfante et al. 2021). The anti-inflammatory effect of AChEIs could be due to attenuation of microglial activation through the p44/42 mitogen-activated protein kinase system (Giunta

et al. 2004). Possibly TVS has neuroprotective properties through inhibitory activity on microglial cells.

As we studied the experimental model of AD, simultaneously with the Nissl stain, we also used the Bielschowsky silver staining method for revealing senile plaques (A β depositions) and neurofibrillary tangles (tau protein), the morphological alterations characteristic of AD (Yamamoto and Hirano 1986; Antonini et al. 2011). By this method, we also studied the morphological state of the entorhinal cortex, which is part of the medial temporal lobe and constitutes the primary gateway between the hippocampal formation and the neocortex (Ibrahim and Hala 2017). Post mortem pathological studies showed that the entorhinal cortex is involved in the early stages of AD development and mild cognitive impairment, thus, this brain region merited special attention in investigating the pathophysiology of AD (deToledo-Morrell et al. 2004; Ibrahim and Hala 2017).

These studies showed that in experimental groups in both regions of the brain, there was a deposition of senile plaques, and some neurons exhibited triangular shape, which corresponded with neurofibrillary tangles. In the hippocampus, after the treatment with TVS, there were more viable cells compared to those in other experimental groups, while in the cortex, the neuroprotective properties of this compound were not obvious. It may be assumed that under the influence of the TVA and TVS, the entorhinal cortex was more susceptible to neuronal injury, although TVS has protected pyramidal neurons of the III layer against A β .

It is known that many AChEI drugs are hepatotoxic; therefore during our experiments we also studied morphological changes in liver tissue (Zhang et al. 2016). The results indicate that the group treated with TVA had signs of acute liver damage, which could contribute to neuronal damage in the hippocampus and entorhinal cortex, as hepatic failure leads to encephalopathy and may contribute to neuronal loss in brain tissue (Lee 2012). There were no signs of liver damage under the influence of TVS, which corresponds to the results of our acute toxicity test. It may

be concluded that TVS is less toxic and can be freely used for pharmacological purposes.

Conclusion

Our research has demonstrated that from among two novel AChE inhibitors tested only TVS has neuroprotective activity. It can be concluded that TVS reduces neurodegeneration induced by A β and may potentially be used in therapeutic treatment to slow down and/or prevent AD development.

Conflicts of interests

The authors have declared that no competing interests exist.

Funding

The study was supported by the RA MES State Committee of Science, Projects No.IST-1D1898 and 21T-3C166.

Dataset deposition

The data underpinning the analysis reported in this paper are deposited at “BioStudies” S-BSST922 at <https://www.ebi.ac.uk/biostudies/studies/S-BSST922>.

Acknowledgments

We thank Dr. John Sarkissian and Dr. Michael Poghosyan from the Laboratory of Central Nervous System Functions Compensation Physiology of LA Orbeli Institute of Physiology NAS RA for the contribution to the design of an animal model of Alzheimer’s disease for experiments.

References

- Abbasi MA, Saeed A, Aziz-Ur-Rehman, Mohmmmed Khan K, Ashraf M, Ejaz SA (2014) Synthesis of brominated 2-phenitidine derivatives as valuable inhibitors of cholinesterases for the treatment of Alzheimer’s disease. *Iranian Journal of Pharmaceutical Research* 13(1): 87–94. [PubMed] [PMC]
- Agatonovic-Kustrin S, Kettleb C, Mortonb DW (2018) A molecular approach in drug development for Alzheimer’s disease. *Biomedicine & Pharmacotherapy* 106: 553–565. <https://doi.org/10.1016/j.biopha.2018.06.147> [PubMed]
- Akhila J, Shyamjith D, Alwar M (2007) Acute toxicity studies and determination of median lethal dose. *Current Science* 93(7): 917–920. <https://doi.org/10.1186/s12906-019-2489-5> [PubMed] [PMC]
- Antonini V, Marrazzo A, Kleiner G, Coradazzi M, Ronisvalle S, Prezzavento O, Ronisvalle G, Leanza G (2011) Anti-amnesic and neuroprotective actions of the sigma-1 receptor agonist (-)-MR22 in rats with selective cholinergic lesion and amyloid infusion. *Journal of Alzheimer’s Disease* 24(3): 569–586. <https://doi.org/10.3233/JAD-2011-101794> [PubMed]
- Bartus RT, Dean 3rd RL, Beer B, Lippa AS (1982) The cholinergic hypothesis of geriatric memory dysfunction. *Science* 217(4558): 408–414. <https://doi.org/10.1126/science.7046051> [PubMed]
- Behl C, Davis JB, Lesley R, Schubert D (1994) Hydrogen peroxide mediates amyloid beta protein toxicity. *Cell* 77(6): 817–827. [https://doi.org/10.1016/0092-8674\(94\)90131-7](https://doi.org/10.1016/0092-8674(94)90131-7) [PubMed]
- Benfante R, Di Lascio S, Cardani S, Fornasari D (2021) Acetylcholinesterase inhibitors targeting the cholinergic anti-inflammatory pathway: a new therapeutic perspective in aging-related disorders. *Aging Clinical and Experimental Research* 33(4): 823–834. <https://doi.org/10.1007/s40520-019-01359-4> [PubMed]
- Bloemer J (2020) Drugs used in the treatment of Alzheimer’s disease. Chapter 5. In: Ray SD (Ed.) *Side Effects of Drugs Annual*. Elsevier, vol. 42: 55–65. <https://doi.org/10.1016/bs.seda.2020.09.003>

- Bradley A, Bertrand L, Rao D, Hall D, Sharma A (2018) Brain in Boorman's Pathology of the Rat. Elsevier, 191–215. <https://doi.org/10.1016/B978-0-12-391448-4.00013-7>
- Chinedu E, Arome D, Ameh FS (2013) A new method for determining acute toxicity in animal models. *Toxicology International* 20(3): 224–226. <https://doi.org/10.4103/0971-6580.121674> [PubMed] [PMC]
- Dani M, Wood M, Mizoguchi R, Fan Z, Walker Z, Morgan R, Hinz R, Biju M, Kuruvilla T, Brooks DJ, Edison P (2018) Microglial activation correlates in vivo with both tau and amyloid in Alzheimer's disease. *Brain* 141 (9): 2740–2754. <https://doi.org/10.1093/brain/awy188> [PubMed]
- da Silva SV, Zhang P, Haberl MG, Labrousse V, Grosjean N, Blanchet C, Frick A, Mulle C (2019) Hippocampal mossy fibers synapses in ca3 pyramidal cells are altered at an early stage in a mouse model of Alzheimer's disease. *Journal of Neuroscience* 39(21): 4193–4205. <https://doi.org/10.1523/JNEUROSCI.2868-18.2019> [PubMed] [PMC]
- deToledo-Morrell L, Stoub T, Bulgakova M, Wilson R, Bennett D, Leurgans S, Wu J, Turner D (2004) MRI-derived entorhinal volume is a good predictor of conversion from MCI to AD. *Neurobiology of Aging* 25(9): 1197–1203. <https://doi.org/10.1016/j.neurobiolaging.2003.12.007> [PubMed]
- Francis PT, Nordberg A, Arnold SE (2005) A preclinical view of cholinesterase inhibitors in neuroprotection: do they provide more than symptomatic benefits in Alzheimer's disease? *Trends in Pharmacological Sciences* 26(2): 104–111. <https://doi.org/10.1016/j.tips.2004.12.010> [PubMed]
- Giunta B, Ehrhart J, Townsend K, Sun N, Vendrame M, Shytle D, Tan J, Fernandez F (2004) Galantamine and nicotine have a synergistic effect on inhibition of microglial activation induced by HIV-1 gp120. *Brain Research Bulletin* 64(2): 165–170. <https://doi.org/10.1016/j.brainresbull.2004.06.008> [PubMed]
- Hampel H, Mesulam MM, Cuello AC, Khachaturian AS, Vergallo A, Farlow MR, Snyder PJ, Giacobini E, Khachaturian ZS (2019) Revisiting the cholinergic hypothesis in Alzheimer's disease: emerging evidence from translational and clinical research. *The Journal of Prevention of Alzheimer's Disease* 6(1): 2–15. <https://doi.org/10.14283/jpad.2018.43> [PubMed]
- Hayes A, Thaker U, Iwatsubo T, Pickering-Brown SM, Mann DM (2002) Pathological relationships between microglial cell activity and tau and amyloid beta protein in patients with Alzheimer's disease. *Neuroscience Letters* 331(3): 171–174. [https://doi.org/10.1016/S0304-3940\(02\)00888-1](https://doi.org/10.1016/S0304-3940(02)00888-1) [PubMed]
- Hemonnot A-L, Hua J, Ulmann L, Hirbec H (2019) Microglia in alzheimer disease: well-known targets and new opportunities. *Frontiers in Aging Neuroscience* 11: 233. <https://doi.org/10.3389/fnagi.2019.00233> [PubMed][PMC]
- Ibrahim KR, Hala ZEM (2017) Histological changes of the adult albino rats entorhinal cortex under the effect of tramadol administration: Histological and morphometric study. *Alexandria Journal of Medicine* 53(2): 123–133. <https://doi.org/10.1016/j.ajme.2016.05.001>
- Jortner BS (2006) The return of the dark neuron. A histological artifact complicating contemporary neurotoxicologic evaluation. *Neurotoxicology* 27(4): 628–634. <https://doi.org/10.1016/j.neuro.2006.03.002> [PubMed]
- Korjevski DE, Gliyarov AV (2010) Basics of histological technique [Osnovy gistologicheskoy tekhniki]. Saint Petersburg, SpecLit, 95 pp. [in Russian]
- Lee WM (2012) Recent developments in acute liver failure. *Best Practice & Research Clinical Gastroenterology* 26(1): 3–16. <https://doi.org/10.1016/j.bpg.2012.01.014> [PubMed] [PMC]
- Leng F, Edison P (2021) Neuroinflammation and microglial activation in Alzheimer disease: where do we go from here? *Nature Reviews Neurology* 17(3): 157–172. <https://doi.org/10.1038/s41582-020-00435-y> [PubMed]
- Makarian M, Gonzalez M, Salvador SM, Lorzadeh S, Hudson PK, Pecic S (2022) Synthesis, kinetic evaluation and molecular docking studies of donepezil-based acetylcholinesterase inhibitors. *Journal of Molecular Structure* 1247: 131425. <https://doi.org/10.1016/j.molstruc.2021.131425> [PubMed] [PMC]
- Maurice T, Su TP, Privat A (1998) Sigma1 (sigma 1) receptor agonists and neurosteroids attenuate B25-35-amyloid peptide-induced amnesia in mice through a common mechanism. *Neuroscience* 83(2): 413–428. [https://doi.org/10.1016/S0306-4522\(97\)00405-3](https://doi.org/10.1016/S0306-4522(97)00405-3) [PubMed] [PMC]
- McGleenon BM, Dynan KB, Passmore AP (1999) Acetylcholinesterase inhibitors in Alzheimer's disease. *British Journal of Clinical Pharmacology* 48(4): 471–480. <https://doi.org/10.1046/j.1365-2125.1999.00026.x>
- Mehta M, Adem A, Sabbagh M (2012) New acetylcholinesterase inhibitors for Alzheimer's disease. *International Journal of Alzheimer's Disease* 2012: 728983. <https://doi.org/10.1155/2012/728983>
- Mesulam M, Shaw P, Mash D, Weintraub S (2004) Cholinergic nucleus basalis tauopathy emerges early in the aging-MCI-AD continuum. *Annals of Neurology* 55(6): 815–828. <https://doi.org/10.1002/ana.20100>
- Mufson EJ, Counts SE, Perez SE, Ginsberg SD (2008) Cholinergic system during the progression of Alzheimer's disease: therapeutic implications. *Expert Review of Neurotherapeutics* 8(11): 1703–1718. <https://doi.org/10.1586/14737175.8.11.1703> [PubMed]
- Ooigawa H, Nawashiro H, Fukui S, Otani N, Osumi A, Toyooka T, Shima K (2006) The fate of Nissl-stained dark neurons following traumatic brain injury in rats: difference between neocortex and hippocampus regarding survival rate. *Acta Neuropathologica* 112(4): 471–481. <https://doi.org/10.1007/s00401-006-0108-2> [PubMed]
- Paxinos G, Watson C (2005) *The rat brain in stereotaxic coordinates*. Elsevier, Academic Press, 5th ed., 367 pp.
- Stuchbury G, Münch G (2005) Alzheimer's associated inflammation, potential drug targets and future therapies. *Journal of Neural Transmission* 112(3): 429–453. <https://doi.org/10.1007/s00702-004-0188-x> [PubMed]
- Tabet N (2006) Acetylcholinesterase inhibitors for Alzheimer's disease: anti-inflammatories in acetylcholine clothing! *Age and Ageing* 35(4): 336–338. <https://doi.org/10.1093/ageing/afk027> [PubMed]
- Topuzyan VO, Kazoyan VM, Tamazyan RA, Aivazyan AG, Galstyan LKh (2018) Synthesis and anticholinesterase activity of [(4Z)-2-Aryl-4-(arylmethylidene)-5-oxo-4,5-dihydro-1H-imidazol-1-yl]alkananoic acids. *Russian Journal of Organic Chemistry* 54: 1369–1377. <https://doi.org/10.1134/S1070428018090178>
- Yamamoto T, Hirano A (1986) A comparative study of modified Bielschowsky, Bodian and thioflavin S stains on Alzheimer's neurofibrillary tangles. *Neuropathology and Applied Neurobiology* 12(1): 3–9. <https://doi.org/10.1111/j.1365-2990.1986.tb00677.x> [PubMed]
- Zhang J, Zhang L, Sun X, Yang Y, Kong L, Lu C, Lv G, Wang T, Wang H, Fu F (2016) AChEI attenuates paracetamol-induced liver injury. *Journal of Pharmacology and Experimental Therapeutics* 359(2): 374–382. <https://doi.org/10.1124/jpet.116.233841>

- Zhang QG, Wang RM, Scott E, Han D, Dong Y, Tu JY, Yang F, Reddy Sareddy G, Vadlamudi RK, Brann DW (2013) Hypersensitivity of the hippocampal CA3 region to stress-induced neurodegeneration and amyloidogenesis in a rat model of surgical menopause. *Brain* 136(Pt 5): 1432–1445. <https://doi.org/10.1093/brain/awt046> [PubMed] [PMC]

Author contributions

- **Hrachik V. Gasparyan**, PhD (Biol.), Head of the Laboratory of Pharmacology and Histopathology, Scientific Technological Center of Organic and Pharmaceutical Chemistry, National Academy of Sciences of the Republic of Armenia; e-mail: hrachikgasparyan@mail.ru; **ORCID ID** <https://orcid.org/0000-0002-8555-3733>. The author had a leading role in planning and conducting the experiments to study the neuroprotective activity of the compounds, and reviewing the manuscript.
- **Sona A. Buloyan**, PhD (Biol.), Senior Researcher at the Laboratory of Pharmacology and Histopathology, Scientific Technological Center of Organic and Pharmaceutical Chemistry, National Academy of Sciences of the Republic of Armenia; e-mail: sonabuloyan@gmail.com; **ORCID ID** <https://orcid.org/0000-0002-6739-509X>. The author performed morphological observations, morphometrical and statistical analyses, and wrote the draft version of the manuscript.
- **Hayk A. Harutyunyan**, PhD (Vet.), Senior Researcher at the Laboratory of Biochemical and Biophysical Investigations, Scientific Research Center, Yerevan State Medical University, Yerevan, Armenia; e-mail: hayk@web.am; **ORCID ID** <https://orcid.org/0000-0001-5674-5130>. The author participated in planning the experiments to study the neuroprotective activity of the substances, analyzing the literature, interpreting the data, and reviewing the manuscript.
- **Anahit E. Pogosyan**, Researcher at the Laboratory of Pharmacology and Histopathology, Scientific Technological Center of Organic and Pharmaceutical Chemistry, National Academy of Sciences of the Republic of Armenia; e-mail: panahit500@gmail.com; **ORCID ID** <https://orcid.org/0000-0001-8776-1483>. The author performed the design and study of acute toxicity of the compounds.
- **Lilit M. Arshakyan**, Junior Researcher at the Laboratory of Pharmacology and Histopathology, Scientific Technological Center of Organic and Pharmaceutical Chemistry, National Academy of Sciences of the Republic of Armenia; e-mail: lmarshakyan@gmail.com; **ORCID ID** <https://orcid.org/0000-0002-1486-5457>. The author participated in studying the neuroprotective activity of the compounds, analyzing the literature, and interpreting the data.
- **Lusine S. Harutyunyan**, Laboratory Assistant at the Laboratory of Pharmacology and Histopathology, Scientific Technological Center of Organic and Pharmaceutical Chemistry, National Academy of Sciences of the Republic of Armenia; e-mail: lus.harutyunyan99@gmail.com; **ORCID ID** <https://orcid.org/0000-0001-8360-9070>. The author participated in studying the neuroprotective activity of the compounds, collecting and preparing the histological tissue samples.
- **Zubeida A. Avetisyan**, PhD (Biol.), Senior Researcher at the Laboratory of Central Nervous System functions compensation Physiology, LA Orbeli Institute of Physiology, National Academy of Sciences of the Republic of Armenia; e-mail: zubeida.avetisyan@gmail.com; **ORCID ID** <https://orcid.org/0000-0002-6177-2552>. The author performed the design of AD experiments, analyzed the literature, and interpreted the data.
- **Syuzanna R. Tosunyan**, PhD (Chem.), Researcher at the Laboratory of Physiologically Active Amino Peptides, Scientific Technological Center of Organic and Pharmaceutical Chemistry, National Academy of Sciences of the Republic of Armenia; e-mail: syuzitos@mail.ru; **ORCID ID** <https://orcid.org/0000-0002-6641-4420>. The author performed the synthesis of the chemical compounds.
- **Armen A. Hovhannisyan**, PhD (Chem.), Senior Researcher at the Laboratory of Physiologically Active Amino Peptides, Scientific Technological Center of Organic and Pharmaceutical Chemistry, National Academy of Sciences of the Republic of Armenia; e-mail: armenarami@gmail.com; **ORCID ID** <https://orcid.org/0000-0003-0879-6800>. The author performed the synthesis of the chemical compounds.
- **Vigen O. Topuzyan**, Prof., Cor.-Member, DSc (Chem.), Head of Laboratory of Physiologically Active Amino Peptides, Scientific Technological Center of Organic and Pharmaceutical Chemistry, National Academy of Sciences of the Republic of Armenia; e-mail: vtop@web.am; **ORCID ID** <https://orcid.org/0000-0002-1721-1993>. The author had a leading role in the planning of the synthesis of the novel chemical compounds.